Since January 2020 Elsevier has created a COVID-19 resource centre with free information in English and Mandarin on the novel coronavirus COVID-19. The COVID-19 resource centre is hosted on Elsevier Connect, the company's public news and information website.

VIROLOGY 244, 483–494 (1998)
ARTICLE NO. VY989121

Roles in Cell-to-Cell Fusion of Two Conserved Hydrophobic Regions in the Murine Coronavirus Spike Protein

Zongli Luo and Susan R. Weiss[1]

Department of Microbiology, University of Pennsylvania School of Medicine, Philadelphia, Pennsylvania 19104-6076

Received December 1, 1997; returned to author for revision February 4, 1998; accepted March 4, 1998

The spike (S) protein of coronavirus, mouse hepatitis virus (MHV), mediates attachment and fusion during viral entry and cell-to-cell fusion later in infection. By analogy with other viral proteins that induce cell fusion the MHV S protein would be expected to have a hydrophobic stretch of amino acids that serves as a fusion peptide. Sequence analysis suggests that the S protein falls within the group of fusion proteins having internal rather than N-terminal fusion peptides. Based on the features of known viral fusion peptides, we identified two regions (PEP1 and PEP2) of MHV-A59 S2 as possible fusion peptides. Site-directed mutagenesis and an *in vitro* cell-to-cell fusion assay were used to evaluate the roles of PEP1 and PEP2, as well as a third previously identified putative fusion domain (PEP3) in membrane fusion. Substitution of bulky hydrophobic residues with charged residues within PEP1 affects the fusion activity of the S protein without affecting processing and surface expression. Similar substitutions within PEP2 result in a fusion-negative phenotype; however, these mutant S proteins also exhibit defects in protein processing and surface expression which likely explain the loss of the ability to induce fusion. Thus PEP1 remains a candidate fusion peptide, while PEP2 may play a significant role in the overall structure or oligomerization of the S protein. PEP3 is an unlikely putative fusion peptide since it is not conserved among coronaviruses and nonconservative amino acid substitutions in PEP3 have minimal effects on cell-to-cell fusion.

INTRODUCTION

Mouse hepatitis virus strain A59 (MHV-A59) is a murine coronavirus with a positive-stranded RNA genome of approximately 31 kb (Siddell *et al.,* 1983). The coronavirus spike (S) protein forms the peplomer structure on the viral envelope; each spike is thought to be a dimer or trimer of S (Cavanagh, 1983). The S protein mediates binding of virions to the host cell receptor (Collins *et al.,* 1982), virus cell fusion during entry, and cell-to-cell fusion at later times postinfection (Vennema *et al.,* 1990). The MHV S protein is cotranslationally glycosylated to a 150-kDa form, which is later processed to a 180-kDa form during intracellular maturation (Spaan *et al.,* 1988). The 180-kDa mature form is cleaved in the Golgi apparatus, by a host cell protease, into two similarly sized subunits: amino terminal S1 and carboxy terminal S2 (Frana *et al.,* 1985; Luytjes *et al.,* 1987; Sturman *et al.,* 1985). It is believed that the S1 subunit forms the globular head of the spike, whereas the S2 subunit forms the membrane-bound stalk portion (de Groot *et al.,* 1987a). Sequence analysis suggests that the coronavirus spike protein has the structural features of a type I membrane protein (Spaan *et al.,* 1988), including a transmembrane domain near the carboxy terminus of S2 and a hydrophobic signal peptide at the N-terminus of S1 Other structural motifs include two heptad repeat domains in S2, the shorter of which is adjacent to the transmembrane domain and is a leucine zipper motif (Britton, 1991). The S1 subunit is believed to interact with receptor (Cavanagh *et al.,* 1986; Taguchi, 1995). A receptor binding activity has been demonstrated using a recombinant protein containing the amino terminal 330 residues of the S1 subunit of MHV-JHM (Kubo *et al.,* 1994). Recombinant S protein, expressed in tissue culture using a vaccinia virus-based expression system, is capable of inducing cell-to-cell fusion (Bos *et al.,* 1995; de Groot *et al.,* 1989), demonstrating that the S protein alone is sufficient for the induction of cell-to-cell fusion. In spite of the important role played by the S protein in viral entry and cell-to-cell fusion, little is known about the fusion domain which is directly responsible for the fusion event.

A common feature of viral fusion proteins is the presence of a fusion peptide, which is believed to participate directly in the fusion process (White, 1992). Fusion peptides are typically composed of 16 to 26 amino acid residues and conserved within, but only rarely among, virus families. They are relatively hydrophobic and generally show an asymmetric distribution of hydrophobicity when modeled into an α helix; they are also rich in alanine and glycine. The majority of known fusion peptides are found at the N-terminus of the membrane-anchored subunit of viral fusion proteins that undergo proteolytic cleavage during their maturation (White, 1990). The cleavage is believed to be necessary in order

[1] To whom correspondence and reprint requests should be addressed. Fax: (215) 573 4858. E-mail: weisssr@mail.med.upenn.edu.

0042-6822/98 $25.00

to expose the peptide itself to facilitate the fusion process. However, not all fusion proteins undergo proteolytic cleavage and there are examples of fusion peptides that exist internally in the membrane-anchored subunit (White, 1990). Besides having the above common features, these internal fusion peptides are bounded by charged residues on both ends and may contain a proline residue in the center.

Although the MHV S protein is cleaved during processing, the N-terminus of the membrane-anchored S2 subunit does not contain a hydrophobic, conserved region. Moreover, not all coronavirus S proteins (for example, feline infectious bronchitis virus and transmissible gastroenteritis virus) undergo cleavage during maturation (Cavanagh, 1995). Thus it is likely that the coronavirus S protein has an internal fusion peptide. Using the properties common to other fusion peptides (discussed above), we have detected two fusion peptide-like regions, PEP1 and PEP2, in the S2 subunit of the MHV-A59 S protein (Fig. 1). We performed mutational analysis of these two regions as well as of a third peptide (PEP3) that was previously proposed as a possible fusion domain (Chambers *et al.,* 1990). The effects of amino acid substitutions within these regions on S-induced cell-to-cell fusion, protein processing, and cell surface expression were examined. The data suggest that mutations in both PEP1 and PEP2 have a dramatic effect on the ability of S to induce cell-to-cell fusion. While mutations in PEP1 have little effect on processing of the S protein, mutations within PEP2 result in the loss of the ability of S to be processed and transported to the plasma membrane. Therefore PEP1 remains a likely candidate fusion peptide, whereas PEP2 may play a role in maintaining the overall structure of S or oligomerization. PEP3 appears unlikely to be a fusion peptide candidate as amino acid substitutions within this peptide have little effect on fusion.

RESULTS

Identification of candidate fusion peptides

Using known characteristics of fusion peptides, including sequence conservation, hydrophobicity, and the ability to be modeled as a sided α helix, we identified two putative fusion peptides, PEP1 and PEP2, in the S2 subunit of the MHV-A59 S protein. Their positions within the S2 subunit are shown in Fig. 1A along with identified functional domains such as the two heptad repeats and the transmembrane domain. PEP1 is located within the longer heptad repeat and PEP2 is located between the two heptad repeats. A third candidate fusion domain, PEP3, previously identified based on its hydrophobicity and its proximity to the heptad repeats (Chambers *et al.,* 1990), is also shown. The MHV-A59 S protein sequence was aligned with those from other coronaviruses using the computer program CLUSTAL V (Higgins *et al.,* 1992). Regions corresponding to PEP1, PEP2, and PEP3 are shown in Fig. 1B. Since coronaviruses are divided into three antigenic groups (Cavanagh, 1995), two representative coronaviruses from groups I (FIPV, TGEV) and II (MHV, BCV) were shown as well as IBV, which is the sole member of group III.

PEP1 shows several of the properties of known fusion peptides. It is conserved among coronaviruses and bordered by charged or polar residues. Most of the unmatched amino acid residues in PEP1 are conservative substitutions. Besides sequence conservation, modeling PEP1 into an α helix shows a clear asymmetric distribution of bulky hydrophobic residues (Fig. 2A). Analysis of the hydrophobicity showed that PEP1 has an overall hydrophobicity index (H.I.) of 0.73. The H.I. for the hydrophobic side is 1.7, while the H.I. for the hydrophilic side is -0.5. PEP1 is rich in alanine and glycine residues (35%). PEP2 also has some features typical of fusion peptides in addition to sequence conservation. For example, PEP2 is bordered by charged residues and showed an asymmetric distribution of hydrophobicity when modeled into an α helix (Fig. 2B). The H.I.s for the hydrophobic and hydrophilic sides are 0.82 and -0.05, respectively. While PEP2 does not have alanine and glycine residues, it contains a central proline residue, another typical feature of internal fusion peptides (White, 1990). Alignment of PEP3 indicates that this region is less conserved than PEP1 and PEP2 (Fig. 1B) among the three antigenic groups of coronaviruses. Furthermore, it is not bordered by charged residues and not predicted to form an α helix with an asymmetric distribution of bulky hydrophobic residues.

Quantitative cell-to-cell fusion assay for the MHV S protein

Using the quantitative fusion assay described in detail under Materials and Methods, we examined the effects of amino acid substitutions on the membrane fusion activity of the S protein. The S gene was expressed in murine DBT cells by infection with vaccinia virus vTF7-3 to supply the T7 RNA polymerase, followed by transfection with a plasmid containing the S gene downstream of a T7 RNA polymerase promoter. Another group of DBT cells was transfected with a plasmid containing the *Escherichia coli lacZ* gene, also downstream of the T7 RNA polymerase promoter. Only when cell fusion occurs between a cell expressing the S gene and a cell containing the lacZ plasmid is the *lacZ* gene transcribed and β-galactosidase subsequently produced. Syncytia were observed and β-galactosidase activities were measured either by an *in situ* assay in which syncytia were stained blue in the presence of 5-bromo-4-chloro-3-indolyl-β-D-galactopyranoside (X-Gal) or by a quantitative assay using CPRG (chlorophenol red-β-D-galactopyranoside) as the substrate (see Materials and Methods). Such an assay is illustrated in Fig. 3. In cells infected with vTF7-3 and mock transfected, only tiny blue background stains

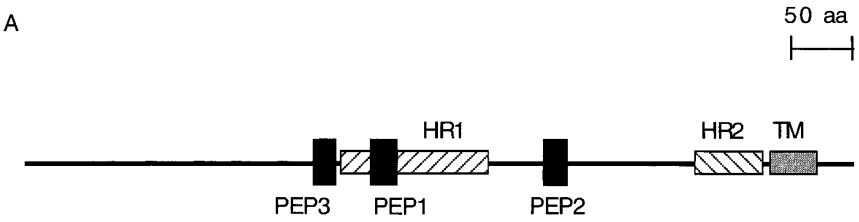

B

PEP1

```
MHV[971-989]          KMIASAFNNALGAIQDGF-D
BCV[1015-1033]        KLIANAFNNALDAIQEGF-D
FIPV[1065-1084]       QILANAFNQAIGNITQAFGK
TGEV[1062-1081]       QILASAFNQAIGNITQSFGK
IBV[796-813]          K-IAASFNKAIGHMQEGF-R
                      . .* .**.*.. . ..* .
```

PEP2

```
MHV[1098-1114]        HILSLVQNAPYGLYFIH
BCV[1142-1158]        HIISLVQNAPYGLYFIH
FIPV[1206-1222]       HLFSLANAAPNGMIFFH
TGEV[1203-1219]       HLFSLANAAPNGMIFFH
IBV[922-938]          HVLTIPQNAPNGIVFIH
                      *.... . ** *. *.*
```

PEP3

```
MHV[929-944]          TGATAAAMFPPWSAAA
BCV[973-988]          LAATSASLFPPWSAAA
FIPV[1022-1037]       ASLAGGITLGALGGGA
TGEV[1019-1034]       ASLAGGITLGALGGGA
IBV[753-768]          SSLVASMAFGGITSAG
                       .  ..  .    ...
```

FIG. 1. Hydrophobic peptides PEP1, PEP2, and PEP3 in the MHV-A59 spike protein S2 subunit. (A) Schematic diagram of S2 showing the relative locations of PEP1, PEP2, and PEP3. The entire S2 subunit of the MHV-A59 S protein is represented by a thin black line. PEP1, PEP2, and PEP3 are represented by the black boxes. The two heptad repeats (HR1 and HR2) in the S2 subunit are represented by hatched boxes. The transmembrane domain is represented by a gray box. (B) Sequence homology of PEP1, PEP2, and PEP3 from different coronaviruses. The S protein sequences of coronaviruses MHV strain A59 (Luytjes *et al.,* 1987), BCV strain F15 (Boireau *et al.,* 1990), IBV strain M41 (Binns *et al.,* 1986), FIPV strain 79-1146 (de Groot *et al.,* 1987b), and TGEV strain TFI (Chen *et al.,* 1993) were aligned by the computer program CLUSTAL V. The regions corresponding to PEP1, PEP2, and PEP3 are shown. Their corresponding positions in the primary sequence are shown in brackets. At the bottom of each alignment, asterisks are used to indicate positions with identical amino acid residues, and a dot for positions with conservative amino acid changes. The positions with nonconservative changes are not indicated by any symbols.

were detected (Fig. 3A). However, in cells infected with vTF7-3 and transfected with plasmid containing the wild-type S gene, fusion of donor cells and the surrounding recipient cells were observed and the resulting syncytia stained blue in the presence of X-Gal (Fig. 3B). The size of the blue stains was equivalent to the size of the induced syncytia (Fig. 3B). The mutant S protein A974D-A976D (described further below) failed to induce fusion, resulting in a fusion phenotype similar to that of mock-transfected cells (Fig. 3C). The fusion-positive mutant S protein S975D (described further below) exhibited a phenotype similar to that of the wild-type S protein (Fig. 3D). The levels of the β-galactosidase activities for the parallel samples were also quantitated to demonstrate that the *in situ* assay reflects the levels of fusion (Fig. 3E). Values indicating the level of fusion were expressed as the percentage of wild-type β-Gal activity after subtracting the background value of mock-transfected cells. The

average size of syncytia usually corresponded to the β-Gal percentage values. A percentage of 0 to 10% indicated a fusion-negative phenotype, while values over 70% of the wild type indicated a fusion phenotype similar to that of the wild type. Values between 10 and 70% indicated intermediate fusion phenotypes.

Analysis of spike proteins with amino acid substitutions in PEP1

To determine the importance of the asymmetric distribution of hydrophobicity in the induction of cell-to-cell fusion, as predicted by the ability to model this peptide as a sided α helix (Fig. 2A), nonconservative and conservative amino acid substitutions were introduced in PEP1 to target representative bulky hydrophobic residues (F977K, F977L, L981K, L981I) and polar or charged residues (S975D, N978D, N978L, D986V-D989V). The importance of the presence of small amino acid residues, such as alanine or glycine, in the mechanism of fusion was tested by substituting them with charged residues (A974D, A976D), bulky hydrophobic residues (A976V), or both at two different positions (A974D-A976D, A974D-A974V).

Since viral fusion proteins undergo complex posttranslational processing before arriving at the cell surface, it is possible that any alteration of the fusogenic ability of the S protein may be caused by defects in protein processing and/or transport rather than to the fusion process itself. Proteins that are defective in processing, for example either misfolded or misassembled, are often retained in the ER and thus not expressed on the cell surface (Doms *et al.,* 1993). Therefore, the level of surface expression is a good indicator as to whether mutant proteins are generally folded correctly. We examined the surface expression of the above PEP1 mutant proteins by flow cytometry analysis to determine whether they were indeed processed and transported to the cell surface. As shown in Fig. 4A, the flow cytometry histogram of the PEP1 mutant A974D-A976D is similar to that of the wild-type S protein. The histograms of all the other PEP1 mutants were similar as well (data not shown). Quantitation of the levels of surface expression (Table 1) indicates that all of the PEP1 mutant S proteins were expressed on the cell surface at levels similar to that of the wild-type S protein, suggesting that their overall conformation was not altered. Thus any alteration of fusion caused by these PEP1 mutations is not likely due to overall conformational changes, but rather likely attributed to a direct influence on the fusion process.

All mutant PEP1 S proteins were assayed for fusion using both *in situ* and quantitative fusion assays, performed as shown in Fig. 3, using the vTF7-3-infected and wild-type S gene-transfected cells as positive controls and vTF7-3-infected and mock-transfected cells as negative controls. The results were summarized in Table 1

TABLE 1

Fusion Activity and Surface Expression of Wild-Type and Various Mutant S Proteins

Construct	Fusion activity[a]	Surface expression[b]
Wild type	100	100
PEP1		
L981I	102	92
L981K	4	87
F977L	96	86
F977K	6	98
N978L	38	92
N978D	44	89
S975D	94	85
D986V–D989V	46	107
A974D	42	103
A976D	57	87
A976V	50	80
A974D–A976D	4	98
A974D–A976V	5	83
PEP2		
L1102K	7	1
V1103K	9	1
P1107K	9	3
L1110K	6	3
I1113K	5	2
PEP3		
M936L	116	ND
M936K	87	ND
P938L	105	ND
P938K	48	ND

[a] Reported as percentage of β-galactoside produced in samples using wild-type S protein (see Materials and Methods). All data are averages of triplicates from one experiment. The experiments were repeated five times with a standard deviation of less than 25%.

[b] Reported as the percentage of the mean fluorescent intensity values measured for samples expressing the wild-type S protein after subtracting background values obtained for mock-transfected samples. Experiments were repeated twice with a standard deviation of less than 20%. ND, Not determined.

Substitution of hydrophobic residues with charged residues generated the fusion negative phenotype. Both F977K and L981K mutations reduced the β-galactosidase activity to the background level. However, replacement of the same residues with other hydrophobic amino acids (F977L, L981I) did not reduce fusion. These results suggest that maintenance of the hydrophobicity at the nonpolar side is important for fusion. Substitution of polar or charged residues on the hydrophilic side of the predicted sided helix had less impact on fusion (Table 1, PEP1). Increasing the hydrophobicity on the polar side (N978L, D986V-D989V) resulted in a partially impaired fusion phenotype. Increasing the hydrophilicity by substituting serine at position 975 with an aspartic acid residue (S975D) did not affect fusion. However, this was not true for the N978D mutant, which failed to maintain the wild-type fusion phenotype. Unlike the serine residue at position 975, this Asn residue is conserved among all coronavirus spike proteins (Fig. 1B). Substitutions of ala-

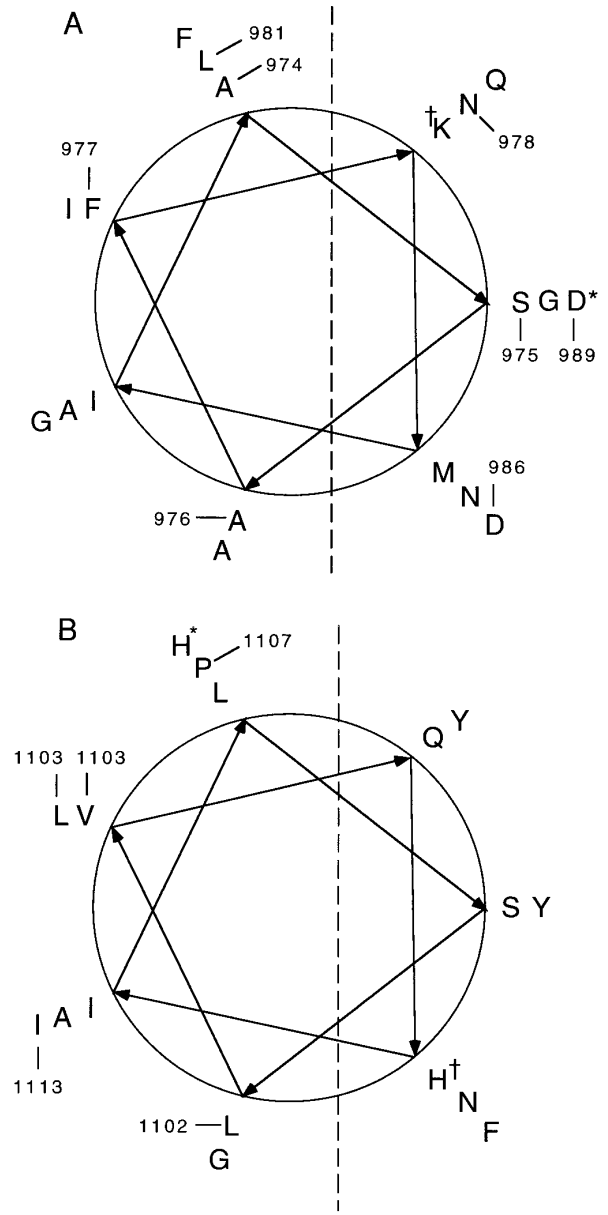

FIG. 2. Schematic diagram of the amino acid sequences of PEP1 and PEP2 as arranged in an α helical wheel. PEP1 (A) and PEP2 (B) are modeled as α helical wheels. The amino acid residues that were subject to mutagenesis are numbered according to their corresponding positions in the primary sequence. The left side of the dotted line indicates the hydrophobic face, while the right side indicates the hydrophilic side. The starting amino acid residue of each wheel is marked by "†", while the ending residue is marked by "*".

nine residues with either a charged residue (A974D or A976D) or a bulky hydrophobic residue (A976V) resulted in a partially reduced fusion phenotype regardless of hydrophobicity. Double mutants A974D-A976D and A974D-A976V both displayed a fusion-negative phenotype, suggesting that the effects of the separate mutation may be additive in the double mutants. The reduced fusion level in A976V mutant S proteins suggests that the alanine residue is required not merely for hydrophobicity. The reduction in fusion observed with the N978D mutant also suggests that conservation at some residues is more of a factor in fusion than hydrophilicity alone.

Mutational analysis of PEP2 and PEP3

PEP2 contains a high percentage of bulky hydrophobic residues and may also be modeled as a sided helix (Fig. 2B). Thus we determined the effect on fusion of substitution of hydrophobic residues on the nonpolar face with the charged lysine residue. All such mutant S proteins appear to have lost the ability to induce fusion (Table 1). Consistent with this, no syncytia were observed in the *in situ* fusion assay. We examined the cell surface expression of PEP2 spike mutants using flow cytometry analysis. Figure 4B demonstrates that, for one representative PEP2 mutant, spike protein is not expressed on the cell surface. Similar results were obtained for all the PEP2 mutants (data not shown); these results are summarized in Table 1. Thus, PEP2 mutant S proteins differed from the PEP1 mutant proteins in that the former were not transported to the cell surface. Therefore, the fusion-negative phenotype of these PEP2 mutants is likely to be an indirect effect of overall conformational changes which prevents transport and expression on the cell surface (Table 1).

To investigate whether the PEP2 mutants were defective in protein transport, they were assayed for endoglycosidase H (endo H) resistance (Fig. 5). During transport from the endoplasmic reticulum (ER) to the Golgi apparatus, glycoproteins are modified by acquisition of oligosaccharides that are resistant to endo H digestion (Kornfeld and Kornfeld, 1985). Proteins that are not processed properly usually fail to gain this resistance. Cells transfected with the plasmids expressing wild-type and PEP2 mutant proteins were labeled with [^{35}S]methionine and cysteine for 1 h and then lysed or labeled and chased with an excess of unlabeled methionine and cysteine before lysis. Proteins were immunoprecipitated with the AO4 anti-S sera, treated with endo H, and analyzed by SDS–PAGE. Endo H resistance was not detectable after 1 h labeling of either wild-type or mutant proteins (Fig. 5A). However, after a 2-h chase, a portion of the wild-type S proteins were processed into an endo H-resistant form (Fig. 5B). These results are consistent with the observation that the processing of S expressed using a vaccinia expression system has a half-time of approximately 3 h (Vennema *et al.,* 1990). Interestingly, the fraction of the wild-type S protein that became endo H resistant is not particularly high. This is similar to the observation made in another study of the MHV-A59 S protein (Bos *et al.,* 1995). Endo H-resistant forms of the PEP2 mutants were not detected even after a 2-h chase, indicating that these mutant proteins were unable to be transported from the ER to the medial

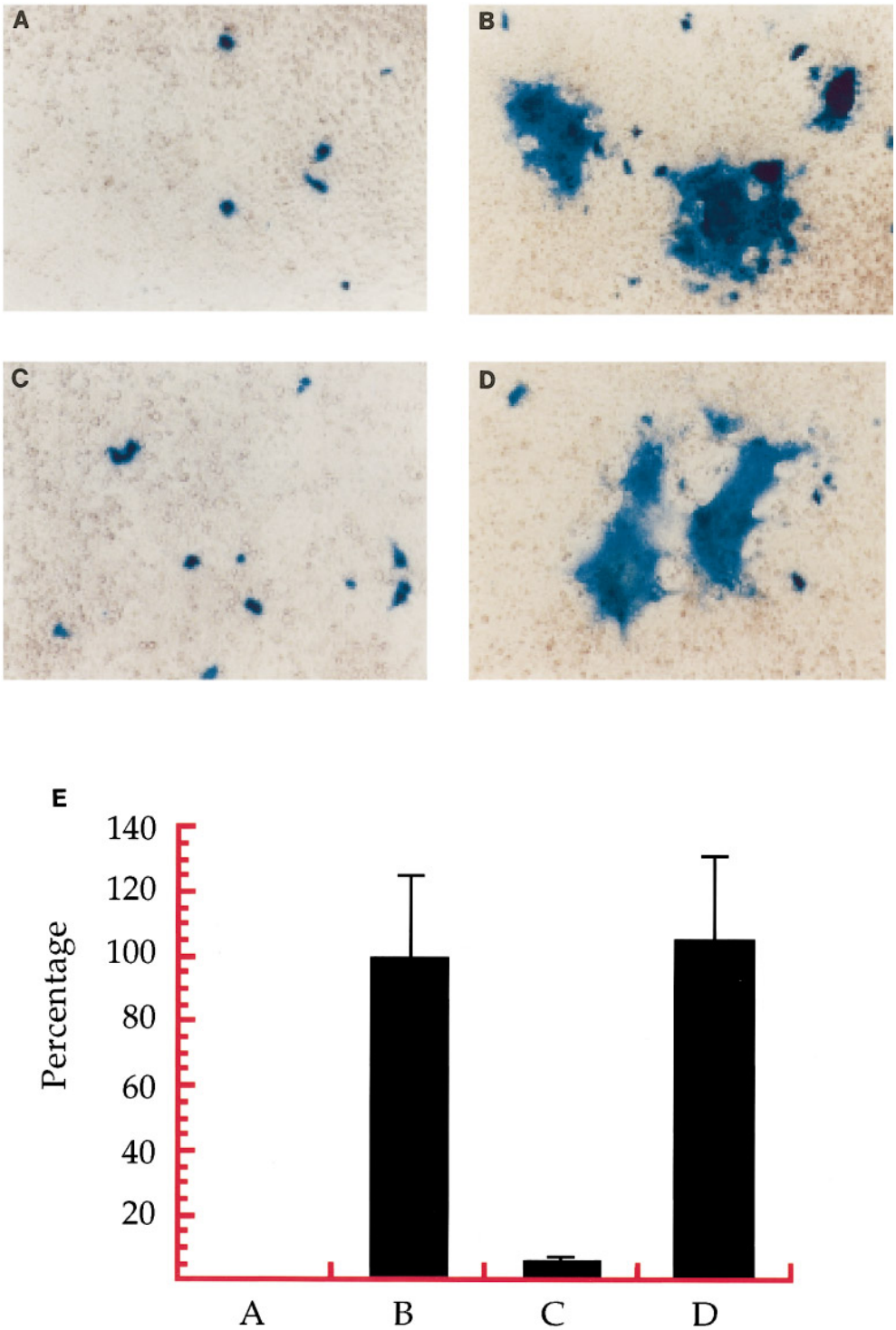

FIG. 3. β-Galactosidase expression and syncytia formation as visualized by the *in situ* assay and quantitated by colorimetric assay. *In situ* assay (A–D) and quantitative colorimetric assay (E) were carried out according to the Materials and Methods. (A) Cells infected with vTF7-3 and mock transfected; (B) cells infected with vTF7-3 and transfected with pINT2 containing the wild-type S gene; (C) cells infected with vTF7-3 and transfected with pINT2 containing the A974D-A976D mutant S gene; (D) cells infected with vTF7-3 and transfected with pINT2 containing the S975D mutant S gene; (E) The production of β-galactosidase from these same samples was quantitated. The vertical axis indicates the percentage of wild-type β-Gal activity after subtracting the background.

Golgi complex. In contrast, an endo H-resistant form of the fusion-negative PEP1 mutant A974D-A976D was detected after a 2-h chase. This protein was also expressed on the cell surface as described above (Table 1), suggesting that correct processing of S correlates with its surface expression.

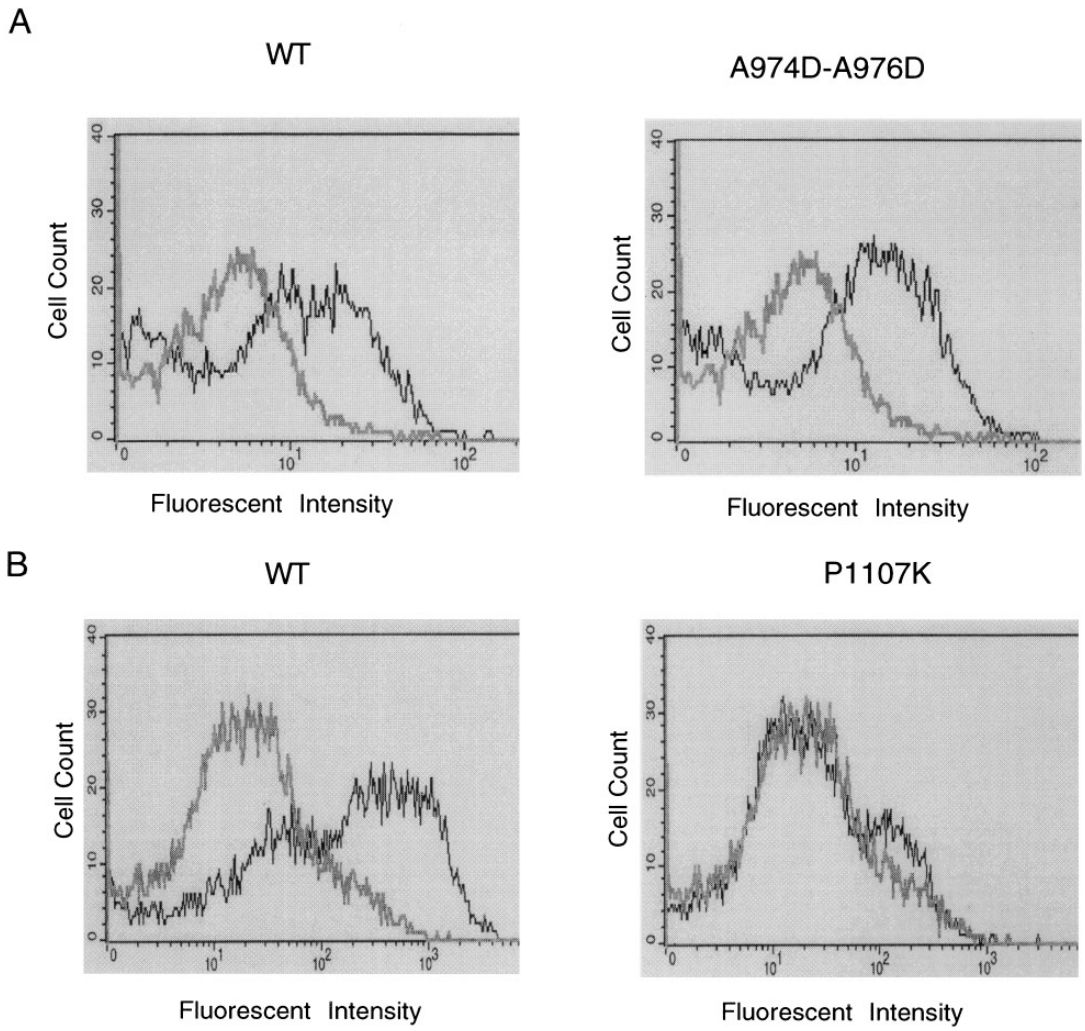

FIG. 4. Flow cytometry analysis of surface expression of wild-type and mutant S proteins. BHK-21 cells were infected with vTF7-3 and transfected with plasmids containing wild-type or mutant S genes. Four hours after transfection, cells were subject to flow cytometry analysis for surface expression of S proteins (see Materials and Methods). Fluorescent histograms of a PEP1 mutant (A974D-A976D) and a PEP2 mutant (P1107K) are shown side by side with the corresponding wild-type controls. Two wild-type controls were shown because A and B represent different experiments. The histogram obtained from a mock-transfected negative control (shown in gray lines) was embedded in each histogram. The *X* axis indicates the arbitrary fluorescent intensity values shown in log scale. The *Y* axis indicates the number of cells. The mean fluorescent intensity values (MFIV) were calculated and the surface expression of each mutant relative to wild type was determined using the following formula: $(MFIV_{sample} - MFIV_{mock})/MFIV_{wild\ type} - MFIV_{mock}) \times 100$.

PEP3 (Fig. 1) was previously proposed as a possible fusion domain based on its hydrophobicity and location adjacent to the heptad repeat domains (Chambers *et al.*, 1990). However, this region is less conserved than PEP1 and PEP2. We performed a limited amount of mutagenesis within this region to determine the effects on fusion. Substitution of the methionine residue at position 936 with lysine (M936K) or leucine (M936L) did not effect fusion. However, while substitution of the proline residue at position 938 with lysine (P938K) partially impaired fusion, replacing the same proline residue with a leucine residue did not have any effect on fusion. The results suggest that PEP3 is unlikely to be a putative fusion peptide.

DISCUSSION

Although studies of the coronavirus S protein reveal that S alone is sufficient to induce cell-to-cell fusion in the absence of other coronavirus proteins, little is known about the fusion peptide domain of the S protein. Using the characteristics of known fusion peptides including the observation that they may be modeled as α helices with an asymmetric distribution of hydrophobicity, we identified two conserved hydrophobic regions, PEP1 and PEP2, in the MHV-A59 S protein S2 subunit, as candidate fusion peptides. Site-directed mutational analysis was used to examine the significance of individual amino acid residues within each of these peptides in cell-to-cell

fusion. A third previously identified peptide was also examined as a possible fusion domain. The mutagenesis results indicate that PEP1 remains the most likely candidate fusion peptide. All PEP1 mutants we analyzed, including the ones that displayed a fusion-negative phenotype, were expressed on the cell surface at a level similar to that of the wild-type protein. In contrast, the group of PEP2 mutants were defective in a step in processing or intracellular transport; thus the negative fusion phenotype was likely due to the lack of expression on the cell surface rather than to a direct effect on the ability to induce cell-to-cell fusion. Mutations in PEP3 had less effect on the fusogenic ability of S; this along with the fact that this domain is not well conserved among coronaviruses makes it an unlikely candidate fusion peptide.

A current hypothesis on how viral fusion proteins induce membrane fusion is that fusion involves a conformational change of fusion proteins which is triggered by low pH or another factor(s) (White, 1992). The altered conformational change allows the hydrophobic fusion peptide to interact with the target membrane. The fusion peptide is postulated to act as a sided insertional helix. The hydrophobic face of the helix inserts into the membrane with an oblique orientation, leading to the disruption of the membrane structure (Harter *et al.,* 1989; White, 1990, 1992). Alteration of this hydrophobic face would affect this interaction. The perturbation of the hydrophobic face in PEP1 by substitution of bulky hydrophobic residues with charged ones may prohibit the insertion, thus abrogating the fusogenic activity. Other less drastic amino acid substitutions may result in less severe obstruction of this type of interaction, thus having less drastic effect on fusion.

PEP1 is located within the longer of the two heptad repeat regions in S2. Since heptad repeat motifs are typical of regions that form α helical coiled coil structures (Cohen and Parry, 1986), it is likely that PEP1 adopts an α helical conformation as part of this coiled coil structure. PEP1 is distinguished from the rest of the heptad repeat region in that it possesses several features common to known viral fusion peptides. Those include sequence conservation among coronaviruses, hydrophobicity, richness in alanine and glycine residues, and the ability to be modeled into a sided helix and bounded by charged residues. Studies of heptad repeat regions in many viral fusion proteins have revealed that they are also essential for membrane fusion (Buckland *et al.,* 1992; Dubay *et al.,* 1992; Sergel-Germano *et al.,* 1994). Although fusion peptides are generally found adjacent to heptad repeats but not within the heptad repeat, there is no indication that fusion peptides cannot reside in a heptad repeat. It is postulated that heptad repeats may also be able to insert into membranes to help elicit fusion because of the amphipathic nature of their helices (Segrest *et al.,*

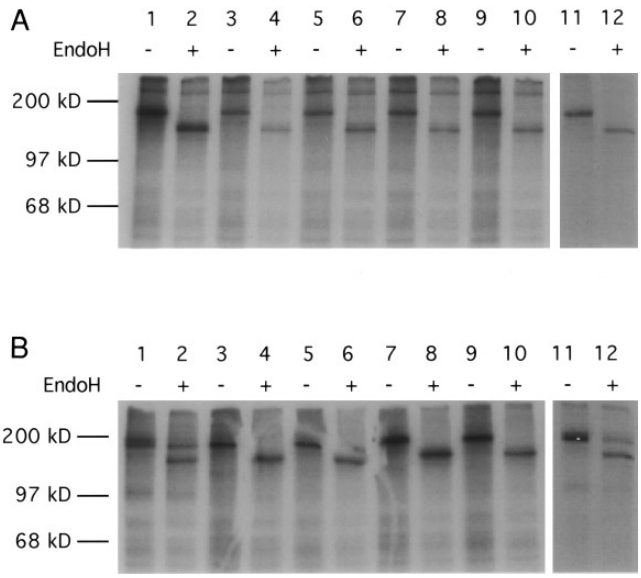

FIG. 5. Endoglycosidase H analysis of the PEP2 mutants. Cells expressing the wild-type or the PEP2 mutant S proteins were metabolically labeled for 1 h with ^{35}S Express Labeling Mix and either analyzed directly (A) or incubated further for 2 h in the presence of excess methionine and cysteine (B). Cells were lysed and S proteins were immunoprecipitated using anti-S AO4 serum. Half of each sample was digested with Endo H_f (+) or incubated without the enzyme (−). Wild-type S gene (lanes 1, 2), L1102K mutant (lanes 3, 4), V1103K mutant (lanes 5, 6), P1107K mutant (lanes 7, 8), L1110K mutant (lanes 9, 10), PEP1 mutant A974D–A976D (lanes 11, 12). The little black spot above the endo H-sensitive spike band in lane 6 was caused by a slight gel crack.

1992; Sergel-Germano *et al.,* 1994). Synthetic peptides representing part of the influenza virus HA heptad repeat region have been shown to insert reversibly into phospholipid vesicles under endosomal pH conditions (Yu *et al.,* 1994). Amphipathic α helices of a protein molecule may associate with membranes spontaneously (DeGrado, 1993; Segrest *et al.,* 1990). Melittin, an amphipathic helical peptide, is capable of inducing membrane fusion due to a local disruption of the lipid bilayer (Dempsey, 1990). Thus, fusion peptides and heptad repeats may be indispensable parts of an integrated fusion machinery whereby fusion peptides may or may not be located independently from heptad repeats.

PEP1 has 35% alanine and glycine residues. Although substitution of one alanine residue by another charged one (A976D) reduced fusion, substitution with a more hydrophobic valine residue (A976V) also reduced fusion, suggesting that alanine residues may have roles in fusion other than the maintenance of hydrophobicity. Replacement of glycine residues by valine residues in the HIV gp41 fusion peptide either abrogated or reduced fusion (Delahunty *et al.,* 1996). It is postulated that the presence of small glycine/alanine residues in the fusion peptide provide the right balance of amphipathicity necessary in mediating fusion for influenza virus (White,

1992). Furthermore, studies on the SIV gp32 fusion peptide suggest that the presence of these residues may be important for oblique insertion of the fusion peptide into the target membrane (Horth *et al.,* 1991).

Substitution of bulky hydrophobic residues with charged lysine residues in all constructed PEP2 mutants abolished the fusogenic ability of S. However, this is likely due to a defect in processing or transport to the cell membrane rather than to a direct effect on the fusion process. The failure to detect an endo H-resistant form of S for the PEP2 mutants (Fig. 5) suggests that this region plays a role in the maturation of S. For example, mutations in PEP2 may cause individual molecules to be misfolded, leading them to form aggregates even before appropriate oligomerization occurs. Such aggregates are normally retained in the ER (Marquardt and Helenius, 1992). Consistent with our data are studies in which Gallagher (1996) demonstrated that membrane fusion induced by the MHV-JHM S protein was inhibited by modification of Cys-1163 and suggested that this was likely due to dramatic changes in S protein structure. Sequence alignment of MHV-JHM and MHV-A59 indicates that this cysteine residue corresponds to a tyrosine residue in MHV-A59, which is located in the PEP2 region. Furthermore, studies of two temperature-sensitive MHV-A59 mutants in which the endo H-resistant form of S was not detectable at nonpermissive temperatures was caused by the lack of oligomerization (Luytjes *et al.,* 1997), albeit the location of these mutations is not known. Appropriate oligomerization of many other viral proteins is required for them to be transported from ER to Golgi, where endo H resistance is obtained (Doms *et al.,* 1993).

We have analyzed the roles of three hydrophobic regions in the MHV-A59 S protein in S-induced cell-to-cell fusion. The results of the mutational analysis indicate that PEP1 is likely to be directly involved in fusion, while PEP2 may play a role in maintenance of structure and/or processing of S. Although this study provides insights into identifying the structural elements of S involved in fusion, the molecular details of the fusion mechanism remains unclear. Mutational analysis of PEP1 and PEP2 indicates only that these regions are necessary for the S protein to assume a fusion competent conformation. Whether either of these two regions is a fusogenic peptide needs to be determined by biophysical studies using liposomes. Similar studies have been conducted on fusion peptides for other proteins such as HIV gp41 (Nieva *et al.,* 1994), influenza virus HA2 (Luneberg *et al.,* 1995), and sperm surface protein PH-30 (Muga *et al.,* 1994). Such biophysical studies of the S protein, together with the elucidation of the three-dimensional structure of S, would greatly help the understanding of the fusion mechanism.

MATERIALS AND METHODS

Mutagenesis of the MHV-A59 spike gene

Plasmid pINT2 contains a cDNA copy of the entire wild-type MHV-A59 S gene, cloned into the *Sac*I and *Bam*H I sites of pBlueScript II (KS^+) (Stratagene), the expression of which is under the control of the T7 RNA polymerase promoter. The *Hin*dIII site of the S gene in pINT2 was modified to an *Ase*I site by the introduction of silent mutations in codons 173 and 174. The mutant S plasmid clones were generated by oligonucleotide-directed PCR mutagenesis (Ausubel *et al.,* 1989), using pINT2 as the template. For the PEP1 or PEP3 region, desired nucleotide changes were introduced into a PCR-amplified fragment using the 5′ flanking primer wz157 (5′-AACACTGCATGCAGGCAG-3′), the 3′ flanking primer wz175 (5′-ATTAATACGCGTGGTTTGGC-3′), and the corresponding mutagenic primers listed in Table 2. The PCR fragments were digested with *Bbs*I and *Mlu*I and cloned into the corresponding sites of pINT2. For the PEP2 mutants, primers wz115 (5′-AGCAAAAGCCCAGATAGA-3′) and wz11 (5′-GGGGGATCCAGGTAGC-3′) were used as the 5′ and 3′ flanking primers, respectively, along with the corresponding mutagenic primers listed in Table 2. The resulting mutant plasmids were generated by subcloning the *Mlu*I–*Nde*I-digested mutant PCR fragments into the corresponding sites of pINT2. The presence of specific mutations in all constructs was verified by DNA sequencing.

Fusion assay

Spike-induced cell-to-cell fusion was examined by using expression of the *E. coli lac*Z gene to monitor the level of fusion, in an assay adapted from Nussbaum *et al.* (1994). Briefly, one group of DBT cells was seeded onto a 96-well plate (Falcon) to be used as donor cells. The second group of DBT cells was seeded into a 80-cm^2 tissue culture flask (Nunclon) as recipient cells. After overnight incubation at 37°C, cells from the donor cell group were infected with vaccinia virus vTF7-3 (Fuerst *et al.,* 1986) at 5 PFU/cell for 1 h at 37°C and then transfected with plasmids (0.2 μg/well) containing either wild-type or mutant S genes using lipofectin (GIBCO/BRL) according to the manufacturer's protocol. The recipient cells were transfected with the plasmid pG1NTβGal (10 μg/flask) containing the *E. coli lac*Z gene under the control of the T7 RNA polymerase promoter (Nussbaum *et al.,* 1994). The efficiency of lipofection in this and all the other experiments described below was 20 ± 5%, as determined by the percentage of blue cells visualized by staining with X-Gal after cells were infected with vTF7-3 and then transfected with pG1NTβGal. After 4 h, the donor cells were washed once with Dulbecco's modified Eagle's medium (DMEM) and resupplied with DMEM. The recipient cells were trypsinized, washed once with

TABLE 2

Oligonucleotides Used for the PCR Mutagenesis

Name	Position[a]	Sequence[b]	Purpose[c]
wz16	2943–2981	GGGTGCTATCCAGGTTGGGTTTGTTGCAACCAATTCTGC	D986V–D989V
wz123	2908–2949	CAAAAGATGATTGCTAGTGCTaagAACAATGCGCTGGGTGCT	F977K
wz124	2920–2963	GCTAGTGCTTTTAACAATGCGaaGGGTGCTATCCAGGATGGGT	L981K
wz111	2904–2940	GAACCAAAAGATGATTGCTgaTGCTTTTAACAATGCG	S975K
wz110	2904–2939	GAACCAAAAGATGATTGaTAGTGCTTTTAACAATGC	A974D
wz17	2904–2939	GAACCAAAAGATGATTGaTAGTGaTTTTAACAATGCG	A974D–A976D
wz153	2920–2964	GCTAGTGCTTTTAACAATGCGaTtGGTGCTATCCAGGATGGG	L981I
wz154	2908–2949	CAAAAGATGATTGCTAGTGCTcTTAACAATGCGCTGGGTGCT	F977L
wz155	2911–2952	AAGATGATTGCTAGTGCTTTTgACAATGCGCTGGGTGCTATC	N978D
wz156	2911–2952	AAGATGATTGCTAGTGCTTTTctCAATGCGCTGGGTGCTATC	N978L
wz162	2905–2946	AACCAAAAGATGATTGCTAGTGaTTTTAACAATGCGCTGGGT	A976D
wz163	2905–2946	AACCAAAAGATGATTGCTAGTGtTTTTAACAATGCGCTGGGT	A976V
wz128	3286–3325	GGTAATCATATATTATCTaagGTCCAGAATGCGCCTTATG	L1102K
wz129	3286–3328	GGTAATCATATATTATCTCTTaagCAGAATGCGCCTTATGGCT	V1103K
wz130	3301–3340	TCTCTTGTCCAGAATGCGaagTATGGCTTATATTTTATAC	P1107K
wz131	3310–3349	CAGAATGCGCCTTATGGCaagTATTTTATACACTTCAGCT	L1110K
wz133	3319–3357	CCTTATGGCTTATATTTTAagCACTTCAGCTATGTGCCA	I1113K
wz158	2785–2826	ACCGGTGCTACTGCGGCAGCTcTGTTCCCACCGTGGTCAGCA	M936L
wz159	2785–2826	ACCGGTGCTACTGCGGCAGCTAaGTTCCCACCGTGGTCAGCA	M936K
wz160	2791–2832	GCTACTGCGGCAGCTATGTTCCtACCGTGGTCAGCAGCTGCC	P938L
wz161	2791–2832	GCTACTGCGGCAGCTATGTTCaagCCGTGGTCAGCAGCTGCC	P938K

[a] The region of the MHV-A59 S sequence covered by each oligonucleotide is marked by the positions of the 5′ and 3′ nucleotides separated by a dash. The position of the 5′ nucleotide is shown first for each oligonucleotide. The positions are numbered in reference to the first nucleotide for the S coding sequence.

[b] Oligonucleotide sequences are shown starting with the 5′ nucleotide. Capital letters indicate that the sequence is exactly the same as the pINT2 sequence. Lowercase letters indicate the mismatched nucleotides designed for specific mutations.

[c] The designated amino acid substitutions resulted from using each mutagenic primer are listed.

DMEM, resuspended in DMEM, plated on top of the donor cell monolayer, and incubated overnight. A 3:1 excess of recipient cells to donor cells was used to ensure that donor cells fuse with the surrounding recipient cells. For the *in situ* staining assay, cells were fixed at 4°C for 5 min with 2% formaldehyde and 0.2% glutaraldehyde. The monolayers were overlaid with X-Gal solution (5 mM potassium ferricyanide, 5 mM potassium ferrocyanide, 2 mM $MgCl_2$, 1 mg/ml X-Gal) and blue stain was observed after incubation at 37°C for 4 h. For quantitation of β-galactosidase activity, cell monolayers were lysed with 1% NP-40. Equal amounts of lysates and CPRG substrate solution (16 mM CPRG, 120 mM $Na_2HPO_4 \cdot 7H_2O$, 80 mM $NaH_2PO_4 \cdot H_2O$, 20 mM KCl, 2 mM $MgSO_4 \cdot 7H_2O$, 10 mM β-mercaptoethanol) were mixed and substrate hydrolysis rates were measured at 570 nm using a microplate absorbance reader (Molecular Devices). The amount of β-galactosidase was calculated using purified *E. coli* β-galactosidase (Boehringer Mannheim) as standard.

Metabolic labeling with [^{35}S]methionine and cysteine

DBT cell monolayers were infected with vTF7-3 at 5 PFU/cell. After 1 h at 37°C, cells were washed once with DMEM and transfected with 2 μg of plasmid containing either wild-type or mutant S genes as described above. After 4 h, cells were washed once with methionine-free DMEM and incubated for 1 h with ^{35}S Express Protein Labeling Mix (110 μCi/ml; NEN/Dupont) in methionine-free DMEM. Cells were either lysed immediately or incubated further for 2 h with DMEM supplemented with excess unlabeled methionine and cysteine (2 mM each) before lysis with ice-cold lysis buffer [50 mM Tris–HCl (pH 7.5), 150 mM NaCl, 0.1% SDS, 1% Nonidet P-40, 0.5% sodium deoxycholate, 10 mM phenylmethylsulfonyl fluoride]. Lysates were centrifuged for 10 min at 13,000 *g* at 4°C to pellet cell debris and nuclei. The supernatants were stored in a −80°C freezer until further analysis.

Immunoprecipitation and endoglycosidase H analysis

For immunoprecipitation, lysates containing equal amounts of radioactive label (4×10^6 TCA-precipitable cpm) were diluted with 1 ml of immunoprecipitation (IP) buffer [50 mM Tris–HCl (pH 7.5), 150 mM NaCl, 0.1 mM EDTA, 0.5% Tween 80, 1 mM phenylmethylsulfonyl fluoride] containing 5 μl of anti-S AO4 goat serum (kindly provided by Dr. K. Holmes, Denver, Colorado) and 30 μl of Protein A–Sepharose 6MB beads (Pharmacia Biotech; diluted 1:1 by the IP buffer). The mixture was incubated overnight at 4°C. Beads were collected by centrifugation and washed twice with 1 ml of ice-cold IP buffer, resuspended in 20 μl of 10 mM Tris · HCl (pH 6.8), 0.4% SDS,

and heated at 95°C for 5 min. Samples were divided into two 10-μl aliquots and mixed with either 10 μl of 50 mM of sodium citrate (pH 5.5) containing 1 mU/μl of Endo H_f (New England Biolabs) or buffer alone. Samples were incubated at 37°C overnight and analyzed by SDS–PAGE (Sambrook *et al.,* 1989). Gels were stained with Coomassie brilliant blue R-250, destained, treated with sodium slicylate (Chamberlain, 1979), dried, and exposed to X-ray film at −80°C.

Surface expression by flow cytometry analysis

Infection with vTF7-3 followed by transfection with 4 μg of plasmid was carried out as above except that BHK-21 cells were used. Four hours after transfection, cells were washed once with DMEM and incubated overnight with DMEM supplemented with 2% fetal bovine serum. Cells were then detached by EDTA, washed once with ice-cold FACS buffer (2% fetal bovine serum diluted in phosphate buffer saline), and resuspended in 100 μl of FACS buffer containing 2 μl of anti-S antibody AO4. After 1 h incubation on ice, the cells were washed twice with cold FACS buffer and then resuspended with 100 μl of FACS buffer containing fluorescein-conjugated rabbit anti-goat IgG (Cappel). The cells were incubated on ice for 1 h, washed twice with cold FACS buffer, and analyzed on a FACSSCAN. The mean fluorescent intensity value for each sample was measured. The surface expression levels of mutant S proteins were expressed as the percentage of the mean fluorescent intensity values for the wild-type S protein after subtracting the background.

ACKNOWLEDGMENTS

This work was supported by NIH Grants NS-21954 and NS-30606. We thank Dr. Kathryn Holmes for the AO4 antiserum and Dr. Bernard Moss for the vTF7-3 vaccinia virus and plasmid pG1NTβGal. We thank Dr. Francisco Gonzalez-Scarano, Dr. Paul Bates, and Joanna Philips for comments on the manuscript.

REFERENCES

Ausubel, F. M., Brent, R., Kingston, R. E., Moore, D. D., Seidman, J. G., Smith, J. A., and Struhl, K. (1989). "Current Protocols in Molecular Biology." Greene and Wiley–Interscience, New York.

Binns, M. M., Boursnell, M. E., Tomley, F. M., and Brown, D. K. (1986). Comparison of the spike precursor sequences of coronavirus IBV strains M41 and 6/82 with that of IBV Beaudette. *J. Gen. Virol.* 67, 2825–2831.

Boireau, P., Cruciere, C., and Laporte, J. (1990). Nucleotide sequence of the glycoprotein S gene of bovine enteric coronavirus and comparison with the S proteins of two mouse hepatitis virus strains. *J. Gen. Virol.* 71, 487–492.

Bos, E. C. W., Heunen, L., Luytjes, W., and Spaan, W. J. M. (1995). Mutational analysis of the murine coronavirus spike protein: effect on cell-to-cell fusion. *Virology* 214, 453–463.

Britton, P. (1991). Coronavirus motif. *Nature* 353, 394.

Buckland, R., Malvoisin, E., Beauverger, P., and Wild, F. (1992). A leucine zipper structure present in the measles virus fusion protein is not required for its tetramerization but is essential for fusion. *J. Gen. Virol.* 73, 1703–1707.

Cavanagh, D. (1983). Coronavirus IBV: Structural characterization of the spike protein. *J. Gen. Virol.* 64, 2577–2583.

Cavanagh, D. (1995). The coronavirus surface glycoprotein. *In* "The Coronaviridae" (S. G. Siddell, Ed.), pp. 73–113. Plenum, New York.

Cavanagh, D., Davis, P. J., Darbyshire, J. H., and Peters, R. W. (1986). Coronavirus IBV: Virus retaining spike glycopolypeptide S2 but not S1 is unable to induce virus-neutralizing or hemagglutination-inhibiting antibody, or induce chicken tracheal protection. *J. Gen. Virol.* 67, 1435–1442.

Chamberlain, J. P. (1979). Fluorographic detection of radioactivity in polyacrylamide gels with the water-soluble fluor, sodium salicylate. *Anal. Biochem.* 98, 132–135.

Chambers, P., Pringle, C. R., and Easton, A. J. (1990). Heptad repeat sequences are located adjacent to hydrophobic regions in several types of virus fusion glycoproteins. *J. Gen. Virol.* 71, 3075–3080.

Chen, C. M., Pocock, D. H., and Britton, P. (1993). Genomic organization of a virulent Taiwanese strain of transmissible gastroenteritis virus. *Adv. Exp. Med. Biol.* 342, 23–28.

Cohen, C., and Parry, D. A. (1986). Alpha helical coiled coils—A widespread motif in proteins. *Trends Biochem. Sci.* 11, 245–248.

Collins, A. R., Knobler, R. L., Powell, H., and Buchmeier, M. J. (1982). Monoclonal antibodies to murine hepatitis virus-4 (strain JHM) define the viral glycoprotein responsible for attachment and cell-cell fusion. *Virology* 119, 358–371.

de Groot, R. J., Luytjes, W., Horzinek, M. C., van der Zeijst, B. A., Spaan, W. J., and Lenstra, J. A. (1987a). Evidence for a coiled-coil structure in the spike proteins of coronaviruses. *J. Mol. Biol.* 196, 963–966.

de Groot, R. J., Maduro, J., Lenstra, J. A., Horzinek, M. C., van der Zeijst, B. A., and Spaan, W. J. (1987b). cDNA cloning and sequence analysis of the gene encoding the peplomer protein of feline infectious peritonitis virus. *J. Gen. Virol.* 68, 2639–2646.

de Groot, R. J., Van Leen, R. W., Dalderup, M. J., Vennema, H., Horzinek, M. C., and Spaan, W. J. (1989). Stably expressed FIPV peplomer protein induces cell fusion and elicits neutralizing antibodies in mice. *Virology* 171, 493–502.

DeGrado, W. F. (1993). Peptide engineering: Catalytic molten globules. *Nature* 365, 488–489.

Delahunty, M. D., Rhee, I., Freed, E. O., and Bonifacino, J. S. (1996). Mutational analysis of the fusion peptide of the human immunodeficiency virus type 1: Identification of critical glycine residues. *Virology* 218, 94–102.

Dempsey, C. E. (1990). The actions of melittin on membranes. *Biochim. Biophys. Acta* 1031, 143–161.

Doms, R. W., Lamb, R. A., Rose, J. K., and Helenius, A. (1993). Folding and assembly of viral membrane proteins. *Virology* 193, 545–562.

Dubay, J. W., Roberts, S. J., Brody, B., and Hunter, E. (1992). Mutations in the leucine zipper of the human immunodeficiency virus type 1 transmembrane glycoprotein affect fusion and infectivity. *J. Virol.* 66, 4748–4756.

Frana, M. F., Behnke, J. N., Sturman, L. S., and Holmes, K. V. (1985). Proteolytic cleavage of the E2 glycoprotein of murine coronavirus: Host-dependent differences in proteolytic cleavage and cell fusion. *J. Virol.* 56, 912–920.

Fuerst, T. R., Niles, E. G., Studier, F. W., and Moss, B. (1986). Eukaryotic transient-expression system based on recombinant vaccinia virus that synthesizes bacteriophage T7 RNA polymerase. *Proc. Natl. Acad. Sci. USA* 83, 8122–8126.

Gallagher, T. M. (1996). Murine coronavirus membrane fusion is blocked by modification of thiols buried within the spike protein. *J. Virol.* 70, 4683–4690.

Harter, C., James, P., Bachi, T., Semenza, G., and Brunner, J. (1989). Hydrophobic binding of the ectodomain of influenza hemagglutinin to membranes occurs through the "fusion peptide". *J. Biol. Chem.* 264, 6459–6464.

Higgins, D. G., Bleasby, A. J., and Fuchs, R. (1992). CLUSTAL V: Improved software for multiple sequence alignment. *Comput. Appl. Biosci.* 8, 189–191.

Horth, M., Lambrecht, B., Khim, M. C., Bex, F., Thiriart, C., Ruysschaert, J. M., Burny, A., and Brasseur, R. (1991). Theoretical and functional analysis of the SIV fusion peptide. *EMBO J.* 10, 2747–2755.

Kornfeld, R., and Kornfeld, S. (1985). Assembly of asparagine-linked oligosaccharides. *Annu. Rev. Biochem.* 54, 631–664.

Kubo, H., Yamada, Y. K., and Taguchi, F. (1994). Localization of neutralizing epitopes and the receptor-binding site within the amino-terminal 330 amino acids of the murine coronavirus spike protein. *J. Virol.* 68, 5403–5410.

Luneberg, J., Martin, I., Nussler, F., Ruysschaert, J. M., and Herrmann, A. (1995). Structure and topology of the influenza virus fusion peptide in lipid bilayers. *J. Biol. Chem.* 270, 27606–27614.

Luytjes, W., Gerritsma, H., Bos, E., and Spaan, W. (1997). Characterization of two temperature-sensitive mutants of coronavirus mouse hepatitis virus strain A59 with maturation defects in the spike protein. *J. Virol.* 71, 949–955.

Luytjes, W., Sturman, L. S., Bredenbeek, P. J., Charite, J., van, d., Zeijst, B. A., Horzinek, M. C., and Spaan, W. J. (1987). Primary structure of the glycoprotein E2 of coronavirus MHV-A59 and identification of the trypsin cleavage site. *Virology* 161, 479–487.

Marquardt, T., and Helenius, A. (1992). Misfolding and aggregation of newly synthesized proteins in the endoplasmic reticulum. *J. Cell Biol.* 117, 505–513.

Muga, A., Neugebauer, W., Hirama, T., and Surewicz, W. K. (1994). Membrane interaction and conformational properties of the putative fusion peptide of PH-30, a protein active in sperm-egg fusion. *Biochemistry* 33, 4444–4448.

Nieva, J. L., Nir, S., Muga, A., Goni, F. M., and Wilschut, J. (1994). Interaction of the HIV-1 fusion peptide with phospholipid vesicles: Different structural requirements for fusion and leakage. *Biochemistry* 33, 3201–3209.

Nussbaum, O., Broder, C. C., and Berger, E. A. (1994). Fusogenic mechanisms of enveloped-virus glycoproteins analyzed by a novel recombinant vaccinia virus-based assay quantitating cell fusion-dependent reporter gene activation. *J. Virol.* 68, 5411–5422.

Sambrook, J., Fritsch, E. F., and Maniatis, T. (1989). "Molecular Cloning: A Laboratory Manual." Cold Spring Harbor Laboratory Press, Cold Spring Harbor, NY.

Segrest, J. P., De, L. H., Dohlman, J. G., Brouillette, C. G., and Anantharamaiah, G. M. (1990). Amphipathic helix motif: Classes and properties. *Proteins* 8, 103–117.

Segrest, J. P., Jones, M. K., De, L. H., Brouillette, C. G., Venkatachalapathi, Y. V., and Anantharamaiah, G. M. (1992). The amphipathic helix in the exchangeable apolipoproteins: A review of secondary structure and function. *J. Lipid Res.* 33, 141–166.

Sergel-Germano, T., McQuain, C., and Morrison, T. (1994). Mutations in the fusion peptide and heptad repeat regions of the Newcastle disease virus fusion protein block fusion. *J. Virol.* 68, 7654–7658.

Siddell, S., Wege, H., and Ter Meulen, V. (1983). The biology of coronaviruses. *J. Gen. Virol.* 64, 761–776.

Spaan, W., Cavanagh, D., and Horzinek, M. C. (1988). Coronaviruses: Structure and genome expression. *J. Gen. Virol.* 69, 2939–2952.

Sturman, L. S., Ricard, C. S., and Holmes, K. V. (1985). Proteolytic cleavage of the E2 glycoprotein of murine coronavirus: Activation of cell-fusing activity of virions by trypsin and separation of two different 90K cleavage fragments. *J. Virol.* 56, 904–911.

Taguchi, F. (1995). The S2 subunit of the murine coronavirus spike protein is not involved in receptor binding. *J. Virol.* 69, 7260–7263.

Vennema, H., Heijnen, L., Zijderveld, A., Horzinek, M. C., and Spaan, W. J. (1990). Intracellular transport of recombinant coronavirus spike proteins: implications for virus assembly. *J. Virol.* 64, 339–346.

White, J. M. (1990). Viral and cellular membrane fusion proteins. *Annu. Rev. Physiol.* 52, 675–697.

White, J. M. (1992). Membrane fusion. *Science* 258, 917–924.

Yu, Y. G., King, D. S., and Shin, Y. K. (1994). Insertion of a coiled-coil peptide from influenza virus hemagglutinin into membranes. *Science* 266, 274–276.